$B^+ \to K^+\nu\bar{\nu}$ excess and DM semi-annihilation

Jongkuk Kim[1,2,3,*] and Pyungwon Ko[2,4,†]

[1]Department of Physics, Chung-Ang University, Seoul 06974, Republic of Korea
[2]Excellence Cluster ORIGINS, Boltzmannstraße 2, D-85748 Garching, Germany
[3]Division of Liberal Studies, Kangwon National University, Samcheok 25913, Republic of Korea
[4]School of Physics, Korea Institute for Advanced Study, 85 Hoegi-ro, Seoul 02455, Republic of Korea

(Received 3 December 2025; accepted 5 March 2026; published 17 April 2026)

In 2023, the Belle II Collaboration announced the observation of the $B^+ \to K^+\nu\bar{\nu}$ decay channel for the first time. This decay channel provides a clean signal with high precision in theoretical calculations. However, we encounter a 2.8σ deviation from the Standard Model prediction. To resolve this excess, we study a scalar dark matter model with local discrete Z_3 symmetry. Assuming dark $U(1)_X \equiv U(1)_{L_\mu - L_\tau}$ symmetry, this $U(1)_{L_\mu - L_\tau}$ symmetry is spontaneously broken into local discrete Z_3 by nonzero vacuum expectation value of dark Higgs boson. Considering a dark Higgs mass is 2 GeV, we can explain the recent $\mathrm{Br}(B^+ \to K^+\nu\bar{\nu})$ excess reported from the Belle II Collaboration and relic abundance at the same time.

DOI: 10.1103/5ygk-bswh

I. INTRODUCTION

In 2023, the Belle II Collaboration reported the observation of the rare decay $B^+ \to K^+\nu\bar{\nu}$, with a branching ratio exceeding the Standard Model (SM) expectation by $\sim 2.8\sigma$ confidence level (C.L) [1],

$$\mathcal{B}(B^+ \to K^+\nu\bar{\nu})_{\mathrm{exp}} = (2.3 \pm 0.7) \times 10^{-5}, \quad (1.1)$$

compared to the SM prediction,

$$\mathcal{B}(B^+ \to K^+\nu\bar{\nu})_{\mathrm{SM}} = (5.58 \pm 0.37) \times 10^{-6}. \quad (1.2)$$

This rare B meson decay has long been recognized as a sensitive probe of physics beyond the SM due to the suppression in the SM and the potential for contributions from new particles or interactions beyond the SM. Although the current statistical significance is not yet sufficient to claim a new discovery, this mild deviation could be an early clue to new physics beyond the SM. A number of ideas have been proposed to interpret it in the context of various BSMs, from effective field theory approaches to concrete (UV-complete) models. Several interpretations of this mild excess have been proposed in the literature, including modifications of the Wilson coefficients [2–6] and three-body decay scenarios such as $B^+ \to K^+\chi\bar{\chi}$ involving a new light particle χ [7–16], as well as other BSM frameworks [17–40]. One tantalizing idea for the Belle II excess is to consider light dark sector for $B^+ \to K^+ +$ (missing energy).

Multiple observations from astrophysical and cosmological experiments strongly indicate the presence of dark matter (DM). The precise measurement of the cosmic microwave background (CMB) by the Planck Collaboration indicates that the total DM relic abundance is given by [41]

$$\Omega_{\mathrm{DM}} h^2 = 0.1200 \pm 0.0012. \quad (1.3)$$

Dark matter has been confirmed only through its gravitational effects, and its particle nature remains unknown. This has prompted extensive theoretical studies focused on identifying viable DM candidates and the production mechanisms that could account for the observed relic abundance. Among various DM models, the weakly interacting massive particle (WIMP) is a well-motivated DM candidate. The relic density of the thermal WIMP DM is determined by thermal freeze-out mechanism. The total WIMP DM annihilation cross section required to obtain the correct relic density is [42]

$$\langle \sigma v \rangle_{\mathrm{tot}} \simeq \frac{1}{(20\ \mathrm{TeV})^2}. \quad (1.4)$$

Connecting these two seemingly unrelated observations, the Belle II excess and the dark matter relic density provides a good opportunity to explore some DM models. In this work, we propose a framework that can simultaneously address the excess observed in $B^+ \to K^+\nu\bar{\nu}$ at Belle II and account

*Contact author: jongkukkim@cau.ac.kr
†Contact author: pko@kias.re.kr

Published by the American Physical Society under the terms of the Creative Commons Attribution 4.0 International license. Further distribution of this work must maintain attribution to the author(s) and the published article's title, journal citation, and DOI. Funded by SCOAP³.

for the observed dark matter relic density through semi-annihilation in local Z_3 scalar DM models. By introducing a suitable mediator connecting the dark sector and SM neutrinos, our model provides an explanation of both phenomena at the same time.

The paper is organized as follows. We review local Z_3 scalar DM model in Sec. II. We study DM phenomenology including relic density and direct detection bound in Sec. III. We explore the Belle II excess and possible solution in local Z_3 scalar DM model in Sec. IV. Let us conclude in Sec. V.

II. LOCAL Z_3 SCALAR DM

The dark $\mathrm{U}(1)_X \equiv \mathrm{U}(1)_{L_\mu - L_\tau}$ is anomaly free, not requiring the introduction of additional chiral fermions [43,44]. In the minimal setup accommodating thermal WIMP DM, one introduces a dark Higgs Φ, along with scalar dark matter candidate, X. The dark Higgs is related to the generation of the Z' boson mass. We assume both the Φ and DM are singlets under the SM gauge group $\mathrm{SU}(3)_C \times \mathrm{SU}(2)_L \times \mathrm{U}(1)_Y$. The charge assignments under the $\mathrm{U}(1)_{L_\mu - L_\tau}$ symmetry for these particles are specified as follows:

$$Q_i(\mu, \nu_\mu, \tau, \nu_\tau, X, \Phi) = (1, 1, -1, -1, Q_X, Q_\Phi). \quad (2.1)$$

The UV-complete Lagrangian is given by

$$\begin{aligned}\mathcal{L} = \mathcal{L}_{\mathrm{SM}} &- \frac{1}{4} Z'^{\mu\nu} Z'_{\mu\nu} \\ &- g_X Z'_\mu (\bar{\ell}_\mu \gamma^\mu \ell_\mu - \bar{\ell}_\tau \gamma^\mu \ell_\tau + \bar{\mu}_R \gamma^\mu \mu_R - \bar{\tau}_R \gamma^\mu \tau_R) \\ &+ D_\mu \Phi^\dagger D^\mu \Phi - \lambda_\Phi \left(\Phi^\dagger \Phi - \frac{v_\Phi^2}{2} \right)^2 \\ &- \lambda_{\Phi H} \left(\Phi^\dagger \Phi - \frac{v_\Phi^2}{2} \right) \left(H^\dagger H - \frac{v^2}{2} \right) + \mathcal{L}_{\mathrm{DM}}, \end{aligned} \quad (2.2)$$

where g_X is the $\mathrm{U}(1)_{L_\mu - L_\tau}$ gauge coupling constant, and $D_\mu = (\partial_\mu + i g_X Q_i Z'_\mu)$ is the covariant derivative.

After $\mathrm{U}(1)_{L_\mu - L_\tau}$ symmetry is spontaneously broken, the dark Higgs is described by

$$\Phi(x) = \frac{1}{\sqrt{2}} (v_\Phi + \phi(x)),$$

where v_Φ is the vacuum expectation value (VEV) of the dark Higgs field. The mass of the dark photon Z' is generated by the nonzero VEV of Φ,

$$m_{Z'} = g_X |Q_\Phi| v_\Phi. \quad (2.3)$$

After acquiring nonzero VEVs in both the SM and $U(1)_{L_\mu - L_\tau}$ symmetry, two CP-even neutral scalar bosons mix with each other through the Higgs portal coupling, $\lambda_{\Phi H}$. We define the mixing matrix O connecting the interaction and mass eigenstates as follows:

$$\begin{pmatrix} \phi \\ h \end{pmatrix} = O \begin{pmatrix} H_1 \\ H_2 \end{pmatrix} \equiv \begin{pmatrix} c_\theta & s_\theta \\ -s_\theta & c_\theta \end{pmatrix} \begin{pmatrix} H_1 \\ H_2 \end{pmatrix}, \quad (2.4)$$

where $s_\theta (c_\theta) \equiv \sin\theta (\cos\theta)$, and (ϕ, h) and (H_1, H_2) are the interaction and mass eigenstates with masses m_{H_i} $(i = 1, 2)$, respectively. The mixing angle θ is defined by

$$\tan 2\theta = \frac{\lambda_{\Phi H} v_\Phi v_H}{\lambda_H v_H^2 - \lambda_\Phi v_\Phi^2}, \quad (2.5)$$

where $v_H \simeq 246$ GeV is the VEV of the SM Higgs. The mass matrix in the interaction basis (ϕ, h) can be expressed in terms of the physical parameters as follows:

$$\begin{aligned} &\begin{pmatrix} 2\lambda_\Phi v_\Phi^2 & \lambda_{\Phi H} v_\Phi v_H \\ \lambda_{\Phi H} v_\Phi v_H & 2\lambda_H v_H^2 \end{pmatrix} \\ &= \begin{pmatrix} m_{H_1}^2 c_\theta^2 + m_{H_2}^2 s_\theta^2 & (m_{H_2}^2 - m_{H_1}^2) c_\theta s_\theta \\ (m_{H_2}^2 - m_{H_1}^2) c_\theta s_\theta & m_{H_1}^2 s_\theta^2 + m_{H_2}^2 c_\theta^2 \end{pmatrix}. \end{aligned} \quad (2.6)$$

Now we can consider m_{H_i} and s_θ as independent parameters. The mixing angle θ is constrained by the SM Higgs invisible decay data. We focus on the small mixing, $\sin\theta \ll 1$. Since our model describes a light dark Higgs scenario with $m_{H_1} < m_{H_2}$, we can consistently assume $|\theta| \ll \pi/4$. Consequently, H_1 (H_2) is predominantly dark-Higgs-like (SM Higgs-like) particle, respectively. We set $m_{H_2} = 125.25$ GeV.

We assume that the kinetic mixing between the Z' and the hypercharge gauge boson B vanishes at a high scale. However, a small mixing between the Z' boson and the SM photon A is generated radiatively. After transforming to the canonical basis of gauge fields, the interaction term is given by

$$\mathcal{L}_\epsilon = -\epsilon_A Z'_\mu J^\mu_{\mathrm{em}}, \quad (2.7)$$

where J^μ_{em} denotes the electromagnetic current. At the one-loop level, the mixing parameter ϵ_A is induced by the diagrams with μ and τ leptons running in the loop,

$$\epsilon_A = -\frac{e g_X}{12\pi^2} \ln\left(\frac{m_\tau^2}{m_\mu^2} \right) \simeq -\frac{g_X}{70}. \quad (2.8)$$

The long-standing discrepancy between the measured and SM predicted values of the muon anomalous magnetic moment, $a_\mu = (g-2)_\mu/2$, has long inspired various new physics scenarios. However, the latest lattice-QCD–based SM prediction [45] suggests that the muon $(g-2)$ anomaly has disappeared. The updated average including the recent

Fermilab result [46] gives

$$\Delta a_\mu = (39 \pm 64) \times 10^{-11}. \tag{2.9}$$

In this model, the contribution of the Z' boson to Δa_μ at the one-loop level can be written as [47–51]

$$\Delta a_\mu = \frac{g_X^2}{4\pi^2}\int_0^1 dx \frac{m_\mu^2 x^2(1-x)}{x^2 m_\mu^2 + (1-x)m_{Z'}^2}. \tag{2.10}$$

In our analysis, we use the Fermilab measurement as an experimental constraint on the model parameter space, in particular, on the gauge coupling g_X and the dark photon mass $m_{Z'}$. We adopt the current upper bounds on the gauge coupling g_X, for which $\Delta a_\mu \simeq 10 \times 10^{-10}$.

Constraints on the $(m_{Z'}, g_X)$ plane are taken into account from measurements of $\Delta N_{\rm eff}$ and from the NA64 experiment. The region $m_{Z'} \lesssim 10$ MeV is excluded by the measurements of $\Delta N_{\rm eff}$. It is noteworthy that the Hubble tension can potentially be alleviated by the presence of a light Z' contributing to a certain amount of dark radiation [52,53].

Neutrino trident production has been experimentally established in neutrino beam experiments such as CHARM-II [54] and CCFR [55]. In the presence of an additional gauge interaction mediated by a muon-philic Z' boson, the cross section for muon neutrino trident scattering, $\nu_\mu N \to \nu_\mu N \mu^+\mu^-$, receives extra constructive contributions [51]. Experimental results are conventionally presented in terms of the ratio

$$R \equiv \frac{\sigma_{Z'+\rm SM}}{\sigma_{\rm SM}}. \tag{2.11}$$

The corresponding measurements from CHARM-II [54], CCFR [55], and NuTeV [56] are given by

$$\frac{\sigma_{\rm CHARM\text{-}II}}{\sigma_{\rm SM}} = 1.58 \pm 0.57, \qquad \frac{\sigma_{\rm CCFR}}{\sigma_{\rm SM}} = 0.82 \pm 0.28,$$
$$\frac{\sigma_{\rm NuTeV}}{\sigma_{\rm SM}} = 0.72^{+1.73}_{-0.72}. \tag{2.12}$$

For all experiments, the quoted uncertainties allow for values of $R < 1$, with the central values reported by CCFR and NuTeV lying below unity. Nevertheless, within the experimental uncertainties, all measurements remain consistent with the SM expectation. As a consequence, neutrino trident production has long provided a stringent constraint on a Z' boson associated with a $U(1)_{L_\mu - L_\tau}$ gauge symmetry, effectively excluding regions of parameter space with a light Z' boson mass $M_{Z'} \lesssim \mathcal{O}(1)$ GeV [51]. If future measurements, neutrino near-detector facilities or forward physics experiments [57,58], are to establish a precise determination with $R < 1$, $U(1)_{L_\mu - L_\tau}$ gauge symmetry would no longer be able to accommodate such a result.

Using the current CCFR bound at the 2σ confidence level, the gauge coupling is constrained to $g_X \lesssim 10^{-3}$ for $m_{Z'} \lesssim 200$ MeV. In early 2024, the NA64 experiment has employed a high-energy muon beam together with a missing energy-momentum technique to search for a light Z' boson [59]. In our model, the relevant signal process is $\mu N \to \mu N Z'$, followed by the invisible decay $Z' \to \bar{\nu}\nu$, which leads to a stringent constraint on the gauge coupling g_X. In the following, we therefore focus on a light gauge boson scenario and fix the benchmark mass to $m_{Z'} = 10$ MeV, restricting our numerical analysis to the region $g_X < 10^{-4}$.

Let us consider complex scalar DM with charge assignments $Q_\Phi = 3$ and $Q_X = 1$; the $U(1)_{L_\mu - L_\tau}$ symmetry is reduced to local discrete Z_3 through the Krauss-Wilczek mechanism [60–63]. The Lagrangian for this is described by

$$\mathcal{L}_{\rm DM} = |D_\mu X|^2 - m_X^2|X|^2 - \lambda_{HX}|X|^2\left(|H|^2 - \frac{v_H^2}{2}\right) - \lambda_{\Phi X}|X|^2\left(|\Phi|^2 - \frac{v_\Phi^2}{2}\right) + \lambda_3(X^3\Phi^\dagger + \text{H.c.}), \tag{2.13}$$

where the last λ_3 term is a new gauge invariant operator specific to the charge assignments $Q_\Phi = 3Q_X$. After $U(1)_{L_\mu - L_\tau} \to Z_3$, the scalar DM can be stable thanks to unbroken local Z_3 symmetry. In our analysis, we mainly focus on the DM semi-annihilation processes, while keeping the λ_{HX} and $\lambda_{\Phi X}$ terms in the Lagrangian for completeness.

The interaction between scalar DM and dark photon is given by

$$\mathcal{L}_{\rm DM} \supset i g_X (X^\dagger \partial_\mu X - X \partial_\mu X^\dagger) Z'^\mu. \tag{2.14}$$

Through these interactions, DMs annihilate into a pair of leptons and neutrinos.

In the following, we examine the decay modes of the dark Higgs boson in detail. We investigate the possible decay channels of the dark Higgs boson. The dark Higgs can decay into a pair of gluons, photons, SM fermions, Z' bosons, and dark matter particles. The decay width of the dark Higgs into a pair of fermions is given by

$$\Gamma(H_1 \to f\bar{f}) = N_C s_\theta^2 \frac{m_f^2 m_{H_1}}{8\pi v_H^2}\left(1 - \frac{4m_f^2}{m_{H_1}^2}\right)^{3/2}\Theta(m_{H_1} - 2m_f). \tag{2.15}$$

The decay width of the dark Higgs into a pair of gluons is written as

$$\Gamma(H_1 \to gg) = s_\theta^2 \frac{\alpha_s^2 m_{H_1}^3}{72\pi^3 v_H^2}\left|\sum_q F_{1/2}(\tau_q)\right|^2, \tag{2.16}$$

where $\tau_q = \frac{4m_q^2}{m_{H_1}^2}$. Here, the sum runs over all SM quarks q in the loop, and the loop function $F_{1/2}(\tau)$ is

$$F_{1/2}(\tau) = -2\tau[1 + (1-\tau)f(\tau)], \tag{2.17}$$

with

$$f(\tau) = \begin{cases} \arcsin^2 \frac{1}{\sqrt{\tau}}, & \tau \geq 1, \\ -\frac{1}{4}\left[\ln \frac{1+\sqrt{1-\tau}}{1-\sqrt{1-\tau}} - i\pi\right]^2, & \tau < 1. \end{cases} \tag{2.18}$$

The decay width into a pair of Z' bosons is given by

$$\Gamma(H_1 \to Z'Z') = \frac{g_X^2 Q_\Phi^2 c_\theta^2}{32\pi} \frac{m_{H_1}^3}{m_{Z'}^2}\left(1 - \frac{4m_{Z'}^2}{m_{H_1}^2} + \frac{12m_{Z'}^4}{m_{H_1}^4}\right). \tag{2.19}$$

The decay width of the dark Higgs into a pair of DM particles is

$$\Gamma(H_1 \to X\bar{X}) = \frac{(\lambda_{\Phi H} v_H s_\theta - \lambda_{\Phi X} v_\Phi c_\theta)^2}{16\pi m_{H_1}} \sqrt{1 - \frac{4m_X^2}{m_{H_1}^2}}. \tag{2.20}$$

Since we focus on the semi-annihilation process, we take $\lambda_{\Phi X} = \lambda_{HX} = 0$. Therefore, the dark Higgs cannot decay into a dark matter pair at the tree level.

To explain the Belle II excess, the dark Higgs mass is required to be ∼2 GeV [9]. A detailed discussion of the Belle II result is presented in Sec. 4. For $m_{H_1} = 2$ GeV, the dominant decay channel for the H_1 into the SM particles will be the gluon pair channel. However, in our model, the branching ratio of the dark Higgs decay H_1 into a Z' pair is almost unity, and Z' subsequently decays into a pair of neutrinos since the Z' mass is lighter than the muon mass. The decay $Z' \to e^+e^-$ is highly suppressed due to the small kinetic mixing, $\epsilon_A \sim -g_X/70 \lesssim \mathcal{O}(10^{-6})$. As a result of this tiny kinetic mixing, the decay width of the Z' boson into an e^+e^- pair is given by

$$\Gamma_{Z' \to e^+e^-} = \frac{(e\epsilon_A)^2 m_{Z'}}{12\pi}\left(1 + \frac{2m_e^2}{m_{Z'}^2}\right)\sqrt{1 - \frac{4m_e^2}{m_{Z'}^2}}. \tag{2.21}$$

This leads to the following branching ratio:

$$\begin{aligned} \mathrm{Br}(Z' \to e^+e^-) &= \frac{\Gamma_{Z' \to e^+e^-}}{\Gamma_{Z' \to \nu_\mu \bar{\nu}_\mu} + \Gamma_{Z' \to \nu_\tau \bar{\nu}_\tau}} \simeq \left(\frac{e\epsilon_A}{g_X}\right)^2 \\ &\simeq 2 \times 10^{-5}. \end{aligned} \tag{2.22}$$

We now discuss the current bounds on the invisible decay of the SM Higgs boson. These bounds are primarily obtained from measurements at the LHC, by the ATLAS and CMS Collaborations, and constrain the branching ratio of the Higgs into invisible final states. Specifically, the ATLAS and CMS combined results [64,65] set an upper limit of

$$\mathrm{Br}(H_2 \to \mathrm{inv.}) \lesssim 0.11 \quad \text{at } 95\%\,\mathrm{C.L.} \tag{2.23}$$

Future collider experiments are expected to further improve these limits. For example, the High-Luminosity LHC (HL-LHC) [66], the Compact Linear Collider (CLIC) [67], the Future Circular Collider in the e^+e^- mode (FCC-ee) [68], and the International Linear Collider (ILC) [69] are projected to reach sensitivities down to

$$\mathrm{Br}(H_2 \to \mathrm{inv.}) \sim 0.001. \tag{2.24}$$

These constraints are crucial for testing models in which the Higgs boson can decay into dark matter or other light dark sector particles current and future bounds on the invisible BR of the SM Higgs boson in Table I.

TABLE I. Current and projected limits on the Higgs invisible decay from the LHC, HL-LHC, ILC, CLIC, and FCC-ee [64–69].

Experiments	$\mathrm{Br}(H_2 \to \mathrm{inv.})$	Refs
LHC	11%	[64,65]
High-Luminosity LHC (HL-LHC)	2.25%	[66]
Compact Linear Collider (CLIC)	0.69%	[67]
Future Circular Collider (FCCee)	0.19%	[68]
International Linear Collider (ILC)	0.16%	[69]

III. DARK MATTER

We begin by examining the production mechanism of DM in the early Universe. In the case of thermal freeze-out DM, its relic abundance can be determined by solving the Boltzmann equation, which takes the form

$$\frac{dY_X}{dx} = -\frac{s(x)\langle\sigma v\rangle_{\mathrm{tot}}}{H(x)}(Y_X^2 - (Y_X^{\mathrm{eq}})^2), \tag{3.1}$$

where $x \equiv m_X/T$, H is the Hubble rate, and Y^{eq} is the equilibrium comoving density.

Once the comoving number density is obtained, the present dark matter relic density is related to it via [70],

$$\Omega_X h^2 = 2.755 \times 10^8 \left(\frac{m_X}{\mathrm{GeV}}\right) Y_X. \tag{3.2}$$

Considering DM self-annihilation only, the DM annihilation cross section into a pair of charged leptons and neutrinos can be expressed as

$$\sigma(s) = \sum_\ell \frac{\kappa_f g_X^4}{12\pi}\beta_f \beta_X \left[\frac{s + 2m_f^2}{(s - m_{Z'}^2)^2 + m_{Z'}^2\Gamma_{Z'}^2}\right], \tag{3.3}$$

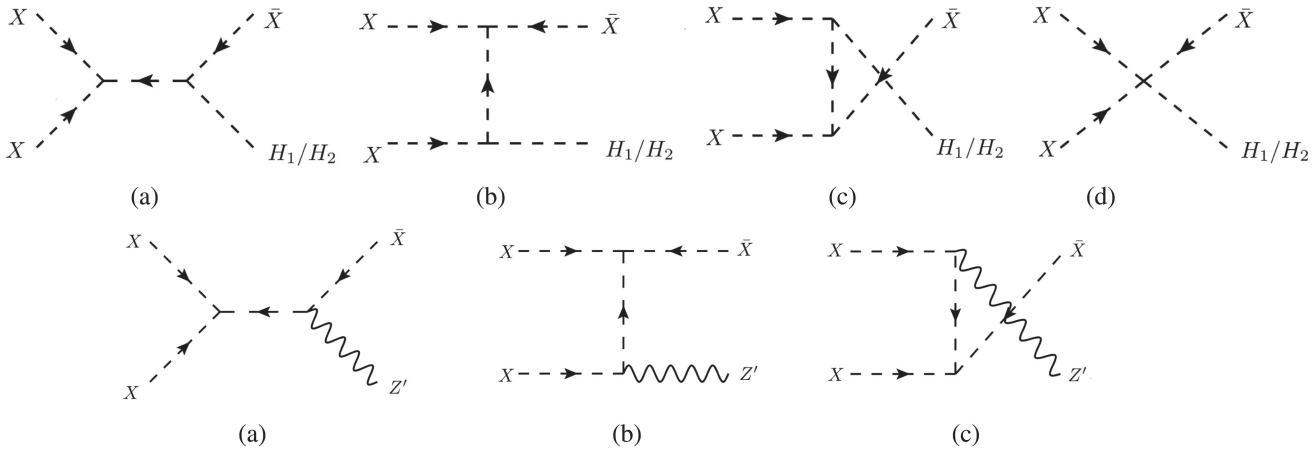


FIG. 1. Feynman diagrams for dark matter semi-annihilation. (Top) Corresponding Feynman diagrams for $XX \to \bar{X}H_{1/2}$.(Bottom) Corresponding Feynman diagrams for $XX \to \bar{X}Z'$.

where $\beta_i = \sqrt{1 - m_i^2/s}$, and $f = \mu, \tau, \nu_\mu, \nu_\tau$. The total decay width of the Z' boson is given by

$$\Gamma_{Z'} = \frac{\kappa_f g_X^2 m_{Z'}}{12\pi}\left(1 + \frac{2m_f^2}{m_{Z'}^2}\right)\sqrt{1 - \frac{4m_f^2}{m_{Z'}^2}}\Theta(m_{Z'} - 2m_f), \tag{3.4}$$

with $\kappa_f = 1$ for $f = \mu, \tau$ and $\kappa_f = 1/2$ for $f = \nu_\mu, \nu_\tau$.

Throughout this study, we take $m_{Z'} = 10$ MeV and assume that the DM particle is always heavier than the Z' boson. Consequently, the decay channel $Z' \to X\bar{X}$ is kinematically forbidden. When the dark Higgs mechanism is not included, the observed relic abundance of DM can be achieved only if $m_{Z'} \simeq m_X/2$, which originates from the smallness of gauge coupling g_X [71–73]. This leads to a strong mass correlation between Z' and DM. A possible way to relax this correlation within the dark Higgs framework has been discussed in Refs. [13,63,74].

In this work, distinctive semi-annihilation channels such as $XX \to \bar{X}H_1$ and $XX \to \bar{X}Z'$ are introduced, in addition to the self-annihilation modes $X\bar{X} \to Z'\phi, Z'h \to$ SM particles [61]. The presence of these extra processes enables a wider viable mass range for the Z_3 complex scalar DM X, thereby alleviating the tight mass correlation $m_X \simeq m_{Z'}/2$ that commonly arises in models where only the Z' mediator is involved and the H_1 field is absent.

We now focus on the scenario in which the DM relic abundance is predominantly governed by semi-annihilation processes in the early Universe because of the smallness of g_X. In contrast to the conventional self-annihilation, semi-annihilation allows one of the final-state particles to remain a DM particle, accompanied by either a SM field or a new light dark-sector state, thereby naturally accounting for the observed relic density. Including such semi-annihilation effects, the Boltzmann equation can be written as

$$\frac{dY_X}{dx} = -\frac{s(x)\langle\sigma v\rangle_{X\bar{X}\to \mathrm{SM}}}{H(x)}(Y_X^2 - (Y_X^{\mathrm{eq}})^2) + \frac{1}{2}\frac{s(x)\langle\sigma v\rangle_{XX\to\bar{X}Y}}{H(x)}(Y_X^2 - Y_X Y_X^{\mathrm{eq}}). \tag{3.5}$$

To realize this setup, we take $\lambda_{XH} = \lambda_{X\Phi} = 0$. Although DM annihilation into lepton pairs remains kinematically accessible, the corresponding annihilation cross section is typically suppressed, except near the resonance region where $m_X \simeq m_{Z'}/2$. The relevant Feynman diagrams are shown in Fig. 1.

The thermal-averaged semi-annihilation cross sections are described by

$$\langle\sigma v\rangle_{XX\to\bar{X}Z'} = \frac{\lambda_3^2}{576\pi m_X^6}\frac{(m_X^2 - m_{Z'}^2)(9m_X^2 - m_{Z'}^2)^3}{(3m_X^2 - m_{Z'}^2)^2}\sqrt{9 - \frac{10m_{Z'}^2}{m_X^2} + \frac{m_{Z'}^4}{m_X^4}} + \mathcal{O}(v^2), \tag{3.6}$$

$$\langle\sigma v\rangle_{XX\to\bar{X}H_1} = \frac{\lambda_3^2}{64\pi}\frac{(s_\theta v_H v_\phi \lambda_{XH}(9m_X^2 + m_{H_1}^2) + c_\theta(3m_X^2(m_{H_1}^2 + 3m_X^2) - \lambda_{X\Phi}v_\Phi^2(m_{H_1}^2 - 9m_X^2)))^2}{m_X^6(3m_X^2 - m_{H_1}^2)^2} \times \sqrt{9 - \frac{10m_{H_1}^2}{m_X^2} + \frac{m_{H_1}^4}{m_X^4}} + \mathcal{O}(v^2). \tag{3.7}$$

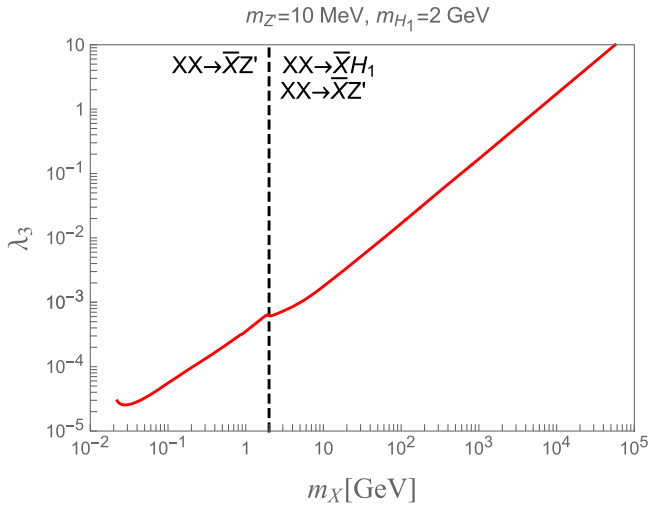


FIG. 2. The relic density in the (m_X, λ_3) plane is shown. We fix $m_{Z'} = 10$ MeV, $m_{H_1} = 2$ GeV, and $\sin\theta = 3 \times 10^{-3}$ to account for the Belle II excess. The impact of varying $\sin\theta$ is negligible due to its small value. The red solid line corresponds to the observed dark matter relic density measured by Planck [41]. To the left (right) of the dashed vertical line, the relic abundance is dominantly determined by the process $XX \to \bar{X}Z'$ ($XX \to \bar{X}Z', \bar{X}H_1$), respectively.

In the heavy DM mass limit and for $\lambda_{XH} = \lambda_{X\Phi} = 0$, the ratio between these semi-annihilations becomes equal due to the Goldstone boson theorem. The related cross section is given by

$$\langle \sigma v \rangle_{XX\to\bar{X}Z'} = \langle \sigma v \rangle_{XX\to\bar{X}H_1} = \frac{27}{64\pi}\frac{\lambda_3^2}{m_X^2}. \tag{3.8}$$

We note that the semi-annihilation cross section is independent of the choice of v_ϕ in this limit. For numerical studies, we make a model file by using FeynRules [75]. Taking into account all of the DM self- and semi-annihilation channels, we obtain the relic density using micrOMEGAs code [76].

In Fig. 2, we show $\Omega_X h^2$ as a function of λ_3 and m_X. The coupling of λ_3 controls the strength of semi-annihilation for different choices of m_X. Given the smallness of the gauge coupling $g_X \le O(10^{-4})$, the semi-annihilation channel $XX \to \bar{X}Z'$ provides significant contribution when $m_X < m_{H_1}$. When $m_X > m_{H_1}$, the process $XX \to \bar{X}H_1$ is kinematically open. We see that the dark Higgs can modify DM phenomenology significantly and the allowed mass range for the complex scalar DM X can significantly deviate from $m_X \sim m_{Z'}/2$ [63].

Although g_X is relatively small, a sizable DM–nucleon elastic scattering cross section can still be obtained compared to Refs. [71–73,77]. This is because a light Z' boson is involved in the t channel of the DM–nucleon scattering process and avoiding the strong mass correlation. The DM–nucleon elastic scattering is given by

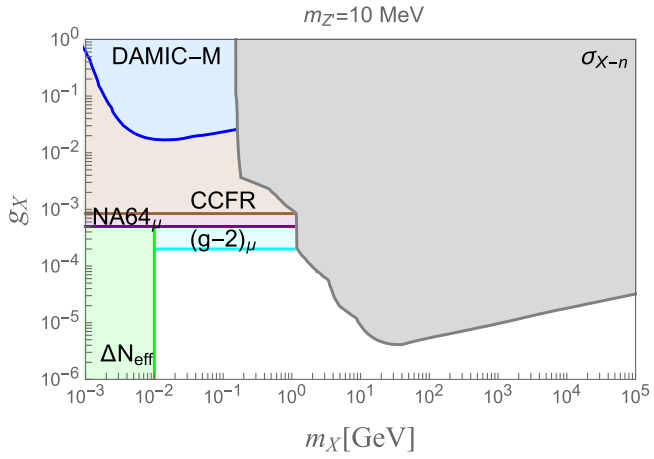


FIG. 3. Allowed (m_X, g_X) space when $m_{Z'} = 10$ MeV. The light brown-shaded region is excluded by the neutrino trident production, $\nu_\mu N \to \nu_\mu N \mu^+\mu^-$, result from CCFR collaboration by 2σ limit [51]. The blue-shaded region is excluded by the DAMIC-M result [79], while the green area is ruled out by the bound $\Delta N_{\rm eff}$. The purple region is excluded by the NA64 [80]. The light-cyan band is disfavored by the latest muon $(g-2)$ measurement at $\Delta a_\mu > 10^{-10}$. Finally, the gray-shaded area is constrained by the current dark matter direct detection limits.

$$\sigma_{\rm el}^{X-n} \simeq \frac{\mu_n^2}{\pi}\frac{e^2 g_X^2 Z^2 \epsilon_A^2}{A^2 m_{Z'}^4}, \tag{3.9}$$

where μ_i is the reduced mass of DM and particle i; A and Z are the number of proton and the nucleus, respectively. When DM mass is above 10 GeV, the most stringent bound on DM-nucleon elastic scattering is from 4.2 Tonne-Years of Exposure of the LUX-ZEPLIN experiment [78]. Similarly, the DM–electron elastic scattering cross section is given by

$$\sigma_{\rm el}^{X-e} \simeq \frac{\mu_e^2}{\pi}\frac{e^2 g_X^2 \epsilon_A^2}{m_{Z'}^4} = \frac{m_e}{\pi m_X}\frac{e^2 g_X^2 \epsilon_A^2}{m_{Z'}^4}, \tag{3.10}$$

where we have used $\mu_e \to m_e/m_X$ when DM mass is much heavier than the electron mass. The current most stringent bound on DM–electron elastic scattering comes from DAMIC-M [79]. We adopted DM–electron bound from DAMIC-M for $m_X < 1$ GeV. The dark matter elastic scattering bounds from LZ (DAMIC) are $\sigma_{\rm el} \sim 10^{-47}(10^{-38})$ cm^2 for dark matter masses of 36 GeV (10 MeV), respectively. After incorporating all experimental bounds, the viable parameter space consistent with Δa_μ in the case of a light Z' is shown in Fig. 3.

In Fig. 3, we depict the allowed parameter space. Here, we take $m_{Z'} = 10$ MeV, and the allowed value of g_X can sustainably relax the Hubble tension [52,53]. The green-shaded area is excluded by $\Delta N_{\rm eff}$ from the Planck observation. The light brown–shaded region is excluded at the 2σ confidence level by the measurement of neutrino trident production, $\nu_\mu N \to \nu_\mu N \mu^+\mu^-$, performed by the CCFR

Collaboration. The observed cross section is consistent with the Standard Model prediction, thereby placing stringent constraints on additional light gauge interactions [51]. The purple region is excluded by NA64$_\mu$ experiment data [80]. Taking into account new SM $(g-2)_\mu$ prediction, the cyan area is ruled out [45]. The blue-shaded region is excluded by the DM–electron scattering bound from DAMIC-M [79]. The gray region is ruled out by the DM direct detection bound on DM–nucleon scattering process by LUX-ZEPLIN [78]. Notice that the viable dark matter mass range strongly depends on the gauge coupling g_X. For $g_X = 10^{-4}$, the dark matter mass is constrained to be below a few GeV. As the coupling decreases to $g_X = 10^{-5}$, the DM mass up to roughly ∼10 GeV is allowed. For even smaller couplings, such as $g_X =$ a few $\times 10^{-6}$, the DM mass can be as large as the unitarity limit, ∼100 TeV. Finally, we briefly discuss the constraint arising from DM annihilation bound at the CMB epoch. Dark matter annihilation during the recombination era, $T \sim$ eV, can inject energy to ionizing particles, which in turn modifies the ionization history of the Universe and affects the temperature and polarization anisotropies of the CMB [81]. These effects are tightly constrained by the most recent Planck satellite observations, which restrict the total amount of energy deposition in that epoch. The constraint is conventionally parametrized as [41]

$$p_{\rm ann} \equiv f_{\rm eff}\frac{\langle\sigma v\rangle}{m_X}, \tag{3.11}$$

where $f_{\rm eff}$ denotes the effective efficiency factor that quantifies the fraction of the annihilation energy deposited into the intergalactic medium. According to the Planck 2018 results, the 95% C.L. upper bound is [41]

$$p_{\rm ann} \lesssim 3.5 \times 10^{-28}\ {\rm cm^3\,s^{-1}\,GeV^{-1}}. \tag{3.12}$$

This constraint can rule out light dark matter scenarios with masses below ∼10 GeV, where DM annihilates into electromagnetically charged final states via the s-wave processes. In the present framework, however, this severe constraint is naturally avoided, since the dark photon Z' and dark Higgs H_1 produced via semi-annihilation predominantly decay into neutrinos.

Previous studies [82,83] have shown that light dark matter annihilating into neutrinos can alter the effective number of relativistic species, $N_{\rm eff}$. In particular, Ref. [83] shows that a complex scalar dark matter with a mass below 8.2 MeV is disfavored due to its impact on the CMB. In this work, we focus on the regime $m_X \gg 10$ MeV, where such constraints are no longer relevant, and thus, the scenario naturally avoids the bound from $N_{\rm eff}$.

IV. BELLE II EXCESS

After the recent announcement from the Belle II collaboration, the measured branching fraction $\mathrm{Br}(B^+ \to K^+\nu\bar{\nu})$ shows a 2.7σ deviation from the SM expectation [1]. The excess observed by Belle II may hint at the presence of new physics beyond the Standard Model. If such new physics contributes to the $b \to s\nu\bar{\nu}$ transition, appearing as missing energy, $\not{E}$, in the final state of the $B^+ \to K^+$ decay, the corresponding branching fraction induced by new physics effects can be written as

$$\mathrm{Br}(B^+ \to K^+\not{E})_{\rm NP} = (1.8 \pm 0.7) \times 10^{-5}. \tag{4.1}$$

Referecne [9] emphasizes that the Belle II analysis provides valuable information on the reconstructed invariant-mass spectrum $q^2_{\rm rec}$, which exhibits a localized enhancement around $q^2_{\rm rec} \simeq 4\ {\rm GeV}^2$. Such a feature can be explained by introducing a new particle with a mass of ∼2 GeV, provided that its couplings to the SM fermions are sufficiently suppressed or absent. Including the null result from *BABAR* data, their combined global analysis yields a branching ratio

$$\mathrm{Br}(B^+ \to K^+ + \chi) = (5.1 \pm 2.1) \times 10^{-6}, \tag{4.2}$$

where χ denotes the new hidden particle. In the case of the two-body decay scenario, the statistical significance decreases to 2.4σ. Therefore, distinct branching ratios are expected between the two-body and three-body decay interpretations. We consider two different branching ratios corresponding to two-body and three-body decays. In particular, Ref. [13] demonstrates that both the observed dark matter relic density and the Belle II excess can be addressed simultaneously within this framework.

First, let us focus on the two-body decay scenario. In this case, the B^+ meson decays into a kaon and a dark Higgs boson, $B^+ \to K^+H_1$. The dark Higgs mass is determined to be $m_{H_1} = 2$ GeV from the observed q^2 spectrum [9]. Such a decay is kinematically allowed when $m_{B^+} - m_{K^+} > m_{H_1}$. Within our framework, the decay width for this two-body decay can be expressed as

$$\Gamma(B^+ \to K^+H_1) \simeq \frac{|\kappa_{cb}|^2\sin^2\theta}{64\pi m^3_{B^+}}[f_0(m^2_{H_1})]^2\left(\frac{m^2_{B^+}-m^2_{K^+}}{m_b-m_s}\right)^2 \times\sqrt{\lambda(m^2_{B^+},m^2_{K^+},m^2_{H_1})}, \tag{4.3}$$

where $\kappa_{cb} \simeq 6.7 \times 10^{-6}$ represents the one-loop induced vertex factor obtained after integrating out the top quark and W boson. The function $f_0(q^2)$, with $q^2 = (p_B - p_K)^2$, denotes the $B^- \to K^-$ transition form factor [84], and $\lambda(a,b,c) \equiv a^2+b^2+c^2-2(ab+bc+ac)$ is the usual Källén function.

Let us now turn to the three-body decay scenario. In this case, the B^+ meson decays via $B^+ \to K^+H_1^{(*)} \to K^+Z'Z'$ or $K^+X\bar{X}$. Since the dark Higgs does not couple directly to the dark matter pair at tree level, it cannot decay into $X\bar{X}$ in the absence of the relevant portal couplings. The decay

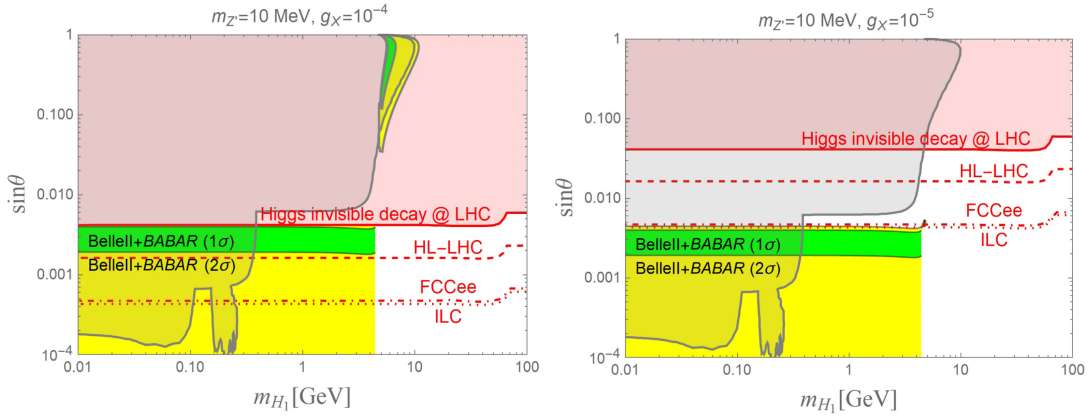


FIG. 4. The regions allowed at the 1σ and 2σ CL by the Belle II excess correspond to the areas enclosed within the green (inner)- and yellow (outer)-shaded bands, respectively. We adopt $g_X = 10^{-4}$ for the left panel and $g_X = 10^{-5}$ for the right panel. The red-shaded region is excluded by the constraint from the invisible decay width of the SM Higgs boson [64,65]. For three-body decay case, the preferred region is already ruled out by the Higgs invisible decay bound. However, the parameter space can be partially reopened when the couplings $\lambda_{X\Phi}$ and/or $\lambda_{H\Phi}$ are nonzero. The gray-shaded area denotes the parameter region excluded by $K^+ \to \pi^+ + \text{inv.}$, $K_L^0 \to \pi^0\nu\bar{\nu}$, and $B^0 \to K^{*0}\nu\bar{\nu}$ [85–87].

width for the process $B^+ \to K^+Z'Z'$ is given by

$$\Gamma(B^+ \to K^+Z'Z') = \frac{|\kappa_{cb}|^2(2g_X Q_\Phi m_{Z'} s_\theta c_\theta)^2}{512\pi^3 m_B^3} \int dm_{23}^2 \times \int dm_{12}^2 \left(3 + \frac{m_{12}^2(m_{12}^2 - 4m_{Z'}^2)}{4m_{Z'}^4}\right) \times \left(\frac{1}{m_{12}^2 - m_{H_1}^2} - \frac{1}{m_{12}^2 - m_{H_2}^2}\right)^2 \times [f_0(m_{12}^2)]^2 \left(\frac{m_{B^+}^2 - m_{K^+}^2}{m_b - m_s}\right)^2. \quad (4.4)$$

When the portal couplings λ_{HX} and $\lambda_{X\Phi}$ are set to zero, the three-body decay channel $B^+ \to K^+H_1^{(*)} \to K^+Z'Z'$ is already excluded by the upper limit on the invisible decay width of the Standard Model Higgs. For nonzero values of λ_{HX} and $\lambda_{X\Phi}$, however, a viable parameter space might remain [13].

In Fig. 4, we show the preferred region of Belle II excess at the 1σ and 2σ confidence levels, shown as the green (inner)- and yellow (outer)-shaded regions, respectively. The left and right panels correspond to $g_X = 10^{-4}$ and $g_X = 10^{-5}$. The red-shaded region is excluded by constraints from the invisible decay width of the Standard Model Higgs boson [64,65]. This bound becomes weaker as the coupling g_X decreases. In the three-body decay scenario, the preferred region is already ruled out by the Higgs invisible decay limit. A portion of the parameter space might be recovered when the couplings $\lambda_{X\Phi}$ and/or $\lambda_{H\Phi}$ are nonzero. Finally, the gray-shaded region represents the parameter space excluded by rare meson decays, including $K^+ \to \pi^+ + \text{inv.}$, $K_L^0 \to \pi^0\nu\bar{\nu}$, and $B^0 \to K^{*0}\nu\bar{\nu}$ [85–87].

V. CONCLUSIONS

Following the announcement of the Belle II excess, a few studies have attempted to simultaneously account for both the observed DM relic density and the $\text{Br}(B^+ \to K^+\nu\bar{\nu})$ excess from Belle II [13,19,28,35]. In most cases, explaining the Belle II excess with light dark matter leads to an excessively large relic abundance due to the requirement of the small coupling. In order to reproduce the observed relic density, it is generally necessary to introduce additional dark matter annihilation channels or allow the dark matter to decay.

In search of a viable solution, we consider a scenario in which the $U(1)_{L_\mu - L_\tau}$ symmetry is broken down to local Z_3 symmetry. Within this framework, two semi-annihilation channels for dark matter are available: $XX \to \bar{X}Z'$ and $XX \to \bar{X}H_1$. By taking a light Z' mass to address the Hubble tension and $m_{H_1} = 2$ GeV to fit the Belle II excess, both the Belle II excess and the correct dark matter relic density can be explained simultaneously. The constraint from the SM Higgs invisible decay depends on the choice of the coupling g_X. For $g_X \lesssim \text{a few} \times 10^{-5}$, even future bounds from the ILC are not expected to exclude the region relevant for the Belle II excess.

Near the Galactic Center (GC), dark matter can undergo semi-annihilation processes, producing light dark sector particles such as Z' and H_1, which subsequently decay into neutrinos. Currently, the IceCube experiment places an upper bound on dark matter annihilation directly into a pair of neutrinos at the level of $\langle\sigma v\rangle_{X\bar{X}\to\nu\bar{\nu}} \sim 10^{-24}\ \text{cm}^3/\text{s}$ [88]. Compared with DM self-annihilation into a pair of neutrinos, the morphology of the produced neutrinos can be different. A dedicated search for neutrinos originating from DM semi-annihilation in the GC would be an interesting possibility,

and we leave a detailed study of this scenario for future work.

ACKNOWLEDGMENTS

The work is supported in part by Basic Science Research Program through the National Research Foundation of Korea (NRF) funded by the Ministry of Education, Science and Technology (Grant No. RS-2024-00341419, J. K.; Grant No. RS-2025-24803289, P. K.) and by KIAS Individual Grant No. PG021403. This research is also supported in part by the Excellence Cluster ORIGINS which is funded by the Deutsche Forschungsgemeinschaft (DFG, German Research Foundation) under Germany's Excellence Strategy–EXC-2094-390783311 (J. K., P. K.).

DATA AVAILABILITY

The data are not publicly available. The data are available from the authors upon reasonable request.

[1] Belle-II Collaboration, Evidence for $B^+ \to K^+\nu\bar{\nu}$ decays, Phys. Rev. D **109**, 112006 (2024).
[2] P. Athron, R. Martinez, and C. Sierra, B meson anomalies and large $B^+ \to K^+\nu\bar{\nu}$ in non-universal $U(1)'$ models, J. High Energy Phys. 02 (2024) 121.
[3] R. Bause, H. Gisbert, and G. Hiller, Implications of an enhanced $B \to K\nu\bar{\nu}$ branching ratio, Phys. Rev. D **109**, 015006 (2024).
[4] L. Allwicher, D. Becirevic, G. Piazza, S. Rosauro-Alcaraz, and O. Sumensari, Understanding the first measurement of $B(B \to K\nu\nu)$, Phys. Lett. B **848**, 138411 (2024).
[5] X.-G. He, X.-D. Ma, and G. Valencia, Revisiting models that enhance $B^+ \to K^+\nu\bar{\nu}$ in light of the new Belle II measurement, Phys. Rev. D **109**, 075019 (2024).
[6] B.-F. Hou, X.-Q. Li, M. Shen, Y.-D. Yang, and X.-B. Yuan, Deciphering the Belle II data on $B \to K\nu\bar{\nu}$ decay in the (dark) SMEFT with minimal flavour violation, J. High Energy Phys. 06 (2024) 172.
[7] A. Berezhnoy and D. Melikhov, $B \to K^* M_X$ vs $B \to K M_X$ as a probe of a scalar-mediator dark matter scenario, Europhys. Lett. **145**, 14001 (2024).
[8] A. Datta, D. Marfatia, and L. Mukherjee, $B \to K\nu\bar{\nu}$, MiniBooNE and muon g-2 anomalies from a dark sector, Phys. Rev. D **109**, L031701 (2024).
[9] W. Altmannshofer, A. Crivellin, H. Haigh, G. Inguglia, and J. Martin Camalich, Light new physics in $B \to K^{(*)}\nu\bar{\nu}$?, Phys. Rev. D **109**, 075008 (2024).
[10] D. McKeen, J. N. Ng, and D. Tuckler, Higgs portal interpretation of the Belle II $B^+ \to K^+\nu\bar{\nu}$ measurement, Phys. Rev. D **109**, 075006 (2024).
[11] K. Fridell, M. Ghosh, T. Okui, and K. Tobioka, Decoding the $B \to K\nu\bar{\nu}$ excess at Belle II: Kinematics, operators, and masses, Phys. Rev. D **109**, 115006 (2024).
[12] K. Cheung, Y. Kim, Y. Kwon, C. J. Ouseph, A. Soffer, and Z. S. Wang, Probing dark photons from a light scalar at Belle II, J. High Energy Phys. 05 (2024) 094.
[13] S.-Y. Ho, J. Kim, and P. Ko, Recent $B^+ \to K^+\nu\bar{\nu}$ excess and muon $g-2$ illuminating light dark sector with Higgs portal, Phys. Rev. D **111**, 055029 (2025).
[14] E. Gabrielli, L. Marzola, K. Müürsepp, and M. Raidal, Explaining the $B^+ \to K^+\nu\bar{\nu}$ excess via a massless dark photon, Eur. Phys. J. C **84**, 460 (2024).
[15] A. Berezhnoy, W. Lucha, and D. Melikhov, Probing vector- vs scalar-mediator dark-matter scenarios in $B \to (K, K^*)M_X$ decays, arXiv:2507.10801.
[16] Q.-Y. Hu and Z.-B. Duan, Influence of invisible light particles on $\Lambda_b \to \Lambda + E_{\rm miss}$, Phys. Rev. D **112**, 095007 (2025).
[17] T. Felkl, A. Giri, R. Mohanta, and M. A. Schmidt, When energy goes missing: New physics in $b \to s\nu\nu$ with sterile neutrinos, Eur. Phys. J. C **83**, 1135 (2023).
[18] Z. S. Wang, H. K. Dreiner, and J. Y. Günther, The decay $B \to K + \nu + \bar{\nu}$ at Belle II and a massless bino in R-parity-violating supersymmetry, Eur. Phys. J. C **85**, 66 (2025).
[19] X.-G. He, X.-D. Ma, M. A. Schmidt, G. Valencia, and R. R. Volkas, Scalar dark matter explanation of the excess in the Belle II $B^+ \to K^+ +$ invisible measurement, J. High Energy Phys. 07 (2024) 168.
[20] P. D. Bolton, S. Fajfer, J. F. Kamenik, and M. Novoa-Brunet, Signatures of light new particles in $B \to K^{(*)} E_{\rm miss}$, Phys. Rev. D **110**, 055001 (2024).
[21] S. Rosauro-Alcaraz and L. P. S. Leal, Disentangling left and right-handed neutrino effects in $B \to K^{(*)}\nu\nu$, Eur. Phys. J. C **84**, 795 (2024).
[22] C. S. Kim, D. Sahoo, and K. N. Vishnudath, Searching for signatures of new physics in $B \to K\nu\bar{\nu}$ to distinguish between Dirac and Majorana neutrinos, Eur. Phys. J. C **84**, 882 (2024).
[23] C. Hati, J. Leite, N. Nath, and J. W. F. Valle, QCD axion, color-mediated neutrino masses, and $B^+ \to K^+ + E_{\rm miss}$ anomaly, Phys. Rev. D **111**, 015038 (2025).
[24] A. J. Buras, J. Harz, and M. A. Mojahed, Disentangling new physics in $K \to \pi\nu\bar{\nu}$ and $B \to K(K^*)\nu\bar{\nu}$ observables, J. High Energy Phys. 10 (2024) 087.
[25] W. Altmannshofer and S. Roy, Joint explanation of the $B \to \pi K$ puzzle and the $B \to K\nu\bar{\nu}$ excess, Phys. Rev. D **111**, 075029 (2025).
[26] Q.-Y. Hu, Are the new particles heavy or light in $b \to s E_{\rm miss}$?, Eur. Phys. J. C **85**, 556 (2025).
[27] W. Altmannshofer, S. A. Gadam, and K. Toner, New strategies for new physics search with $\Lambda_b \to \Lambda\nu\bar{\nu}$ decays, Phys. Rev. D **111**, 075005 (2025).
[28] L. Calibbi, T. Li, L. Mukherjee, and M. A. Schmidt, Is dark matter the origin of the $B \to K\nu\bar{\nu}$ excess at Belle II?, Phys. Rev. D **112**, 075020 (2025).

[29] J.-P. Lee, New physics effects in $R(K^{(*)})$, $B_s \to \mu^+\mu^-$, and $B^+ \to K^+\nu\bar{\nu}$, arXiv:2502.06370.
[30] X.-G. He, X.-D. Ma, J. Tandean, and G. Valencia, $B \to K+$ invisible, dark matter, and CP violation in hyperon decays, J. High Energy Phys. 07 (2025) 078.
[31] A. Berezhnoy, W. Lucha, and D. Melikhov, Analysis of $q^2_{\rm rec}$-distribution for $B \to KM_X$ and $B \to K^*M_X$ decays in a scalar-mediator dark-matter scenario, Phys. Rev. D **111**, 075035 (2025).
[32] P. D. Bolton, S. Fajfer, J. F. Kamenik, and M. Novoa-Brunet, Impact of new invisible particles on $B \to K^{(*)}E_{\rm miss}$ observables, Phys. Rev. D **112**, 035010 (2025).
[33] T. M. Aliev, A. Elpe, L. Selbuz, and I. Turan, Explaining Belle data on $B \to K\nu\bar{\nu}$ decays via dark Z resonances, Phys. Rev. D **112**, 015025 (2025).
[34] C.-H. Chen, C.-W. Chiang, and L. M. G. de la Vega, Leptoquark-mediated Dirac neutrino mass and its impact on $B \to K\nu\bar{\nu}$ and $K \to \pi\nu\bar{\nu}$ decays, J. High Energy Phys. 09 (2025) 055.
[35] K. Ding, Y. Li, X. Liu, Y. Liu, C.-T. Lu, and B. Zhu, Resonant ALP-portal dark matter annihilation as a solution to the $B^\pm \to K^\pm\nu\bar{\nu}$ Excess, arXiv:2504.00383.
[36] X.-G. He, X.-D. Ma, J. Tandean, and G. Valencia, Light dark-matter window constrained by $K^+ \to \pi^+ + E$, Phys. Rev. D **112**, 055025 (2025).
[37] L. Di Luzio, M. Nardecchia, and C. Toni, Gauged τ-lepton chiral currents and $B \to K^{(*)}E_{\rm miss}$, Phys. Rev. D **112**, 055031 (2025).
[38] A. Shaw, Belle II constraints on the non-minimal universal extra dimensional model, arXiv:2509.20027.
[39] A. Berezhnoy, W. Lucha, and D. Melikhov, Scrutinizing dark-matter scenarios with $B \to (K, K^*)\bar{\nu}\nu$ decays, arXiv:2509.23210.
[40] J.-P. Lee, $\Lambda_b \to \Lambda^{(*)}\nu\bar{\nu}$ and $b \to sB$ decays, arXiv:2509.26370.
[41] Planck Collaboration, Planck 2018 results. VI. Cosmological parameters, Astron. Astrophys. **641**, A6 (2020).
[42] G. Steigman, B. Dasgupta, and J. F. Beacom, Precise relic WIMP abundance and its impact on searches for dark matter annihilation, Phys. Rev. D **86**, 023506 (2012).
[43] X. G. He, G. C. Joshi, H. Lew, and R. R. Volkas, New Z-prime phenomenology, Phys. Rev. D **43**, 22 (1991).
[44] X.-G. He, G. C. Joshi, H. Lew, and R. R. Volkas, Simplest Z-prime model, Phys. Rev. D **44**, 2118 (1991).
[45] R. Aliberti *et al.*, The anomalous magnetic moment of the muon in the standard model: An update, Phys. Rep. **1143**, 1 (2025).
[46] Muon g-2 Collaboration, Measurement of the positive muon anomalous magnetic moment to 127 ppb, Phys. Rev. Lett. **135**, 101802 (2025).
[47] S. Baek, N. G. Deshpande, X. G. He, and P. Ko, Muon anomalous $g-2$ and gauged $L_\mu - L_\tau$ models, Phys. Rev. D **64**, 055006 (2001).
[48] K. R. Lynch, Extended electroweak interactions and the muon $g-2$, Phys. Rev. D **65**, 053006 (2002).
[49] E. Ma, D. P. Roy, and S. Roy, Gauged $L_\mu - L_\tau$ with large muon anomalous magnetic moment and the bimaximal mixing of neutrinos, Phys. Lett. B **525**, 101 (2002).
[50] S. Baek and P. Ko, Phenomenology of $U(1)_{L_\mu - L_\tau}$ charged dark matter at PAMELA and colliders, J. Cosmol. Astropart. Phys. 10 (2009) 011.
[51] W. Altmannshofer, S. Gori, M. Pospelov, and I. Yavin, Neutrino trident production: A powerful probe of new physics with neutrino beams, Phys. Rev. Lett. **113**, 091801 (2014).
[52] A. Kamada and H.-B. Yu, Coherent propagation of PeV neutrinos and the dip in the neutrino spectrum at IceCube, Phys. Rev. D **92**, 113004 (2015).
[53] M. Escudero, D. Hooper, G. Krnjaic, and M. Pierre, Cosmology with a very light $L_\mu - L_\tau$ gauge boson, J. High Energy Phys. 03 (2019) 071.
[54] CHARM-II Collaboration, First observation of neutrino trident production, Phys. Lett. B **245**, 271 (1990).
[55] CCFR Collaboration, Neutrino tridents and W Z interference, Phys. Rev. Lett. **66**, 3117 (1991).
[56] NuTeV Collaboration, Evidence for diffractive charm production in muon-neutrino Fe and anti-muon-neutrino Fe scattering at the Tevatron, Phys. Rev. D **61**, 092001 (2000).
[57] P. Ballett, M. Hostert, S. Pascoli, Y. F. Perez-Gonzalez, Z. Tabrizi, and R. Zukanovich Funchal, Neutrino trident scattering at near detectors, J. High Energy Phys. 01 (2019) 119.
[58] W. Altmannshofer, T. Mäkelä, S. Sarkar, S. Trojanowski, K. Xie, and B. Zhou, Discovering neutrino tridents at the large hadron collider, Phys. Rev. D **110**, 072018 (2024).
[59] Y. M. Andreev *et al.*, Exploration of the muon $g-2$ and light dark matter explanations in NA64 with the CERN SPS high energy muon beam, arXiv:2401.01708.
[60] P. Ko and Y. Tang, Galactic center γ-ray excess in hidden sector DM models with dark gauge symmetries: local Z_3 symmetry as an example, J. Cosmol. Astropart. Phys. 01 (2015) 023.
[61] P. Ko and Y. Tang, Self-interacting scalar dark matter with local Z_3 symmetry, J. Cosmol. Astropart. Phys. 05 (2014) 047.
[62] P. Ko and Y. Tang, Semi-annihilating Z_3 dark matter for XENON1T excess, Phys. Lett. B **815**, 136181 (2021).
[63] S. Baek, J. Kim, and P. Ko, Muon $(g-2)$ and thermal WIMP DM in $U(1)_{L_\mu - L_\tau}$ models, J. High Energy Phys. 01 (2025) 014.
[64] ATLAS Collaboration, Combination of searches for invisible decays of the Higgs boson using 139 fb^{-1} of proton-proton collision data at $\sqrt{s} = 13$ TeV collected with the ATLAS experiment, Phys. Lett. B **842**, 137963 (2023).
[65] CMS Collaboration, A search for decays of the Higgs boson to invisible particles in events with a top-antitop quark pair or a vector boson in proton-proton collisions at $\sqrt{s} = 13$ TeV, Eur. Phys. J. C **83**, 933 (2023).
[66] M. Cepeda *et al.*, Report from working group 2: Higgs physics at the HL-LHC and HE-LHC, CERN Yellow Rep. Monogr. **7**, 221 (2019).
[67] CLICdp and CLIC Collaborations, The compact linear collider (CLIC)—2018 summary report, CERN Yellow Rep. Monogr. **2**, 1 (2018).

[68] A. Blondel and P. Janot, FCC-ee overview: New opportunities create new challenges, Eur. Phys. J. Plus **137**, 92 (2022).
[69] C. Potter, A. Steinhebel, J. Brau, A. Pryor, and A. White, Expected sensitivity to invisible Higgs boson decays at the ILC with the SiD detector, arXiv:2203.08330.
[70] J. Edsjo and P. Gondolo, Neutralino relic density including coannihilations, Phys. Rev. D **56**, 1879 (1997).
[71] P. Foldenauer, Light dark matter in a gauged $U(1)_{L_\mu - L_\tau}$ model, Phys. Rev. D **99**, 035007 (2019).
[72] I. Holst, D. Hooper, and G. Krnjaic, The simplest and most predictive model of muon $g-2$ and thermal dark matter, arXiv:2107.09067.
[73] M. Drees and W. Zhao, $U(1)_{L_\mu - L_\tau}$ for light dark matter, $g_\mu - 2$, the 511 keV excess and the Hubble tension, Phys. Lett. B **827**, 136948 (2022).
[74] S. Baek, J. Kim, and P. Ko, XENON1T excess in local Z_2 DM models with light dark sector, Phys. Lett. B **810**, 135848 (2020).
[75] A. Alloul, N. D. Christensen, C. Degrande, C. Duhr, and B. Fuks, FeynRules 2.0—A complete toolbox for tree-level phenomenology, Comput. Phys. Commun. **185**, 2250 (2014).
[76] G. Alguero, G. Belanger, F. Boudjema, S. Chakraborti, A. Goudelis, S. Kraml, A. Mjallal, and A. Pukhov, micrOMEGAs 6.0: N-component dark matter, Comput. Phys. Commun. **299**, 109133 (2024).
[77] J.-C. Park, J. Kim, and S. C. Park, Galactic Center GeV gamma-ray excess from dark matter with gauged lepton numbers, Phys. Lett. B **752**, 59 (2016).
[78] LZ Collaboration, Dark matter search results from 4.2 tonne-years of exposure of the LUX-ZEPLIN (LZ) experiment, Phys. Rev. Lett. **135**, 011802 (2025).
[79] DAMIC-M Collaboration, Probing benchmark models of hidden-sector dark matter with DAMIC-M, Phys. Rev. Lett. **135**, 071002 (2025).
[80] NA64 Collaboration, First results in the search for dark sectors at NA64 with the CERN SPS high energy muon beam, Phys. Rev. Lett. **132**, 211803 (2024).
[81] T. R. Slatyer, Indirect dark matter signatures in the cosmic dark ages. I. Generalizing the bound on Z'-wave dark matter annihilation from Planck results, Phys. Rev. D **93**, 023527 (2016).
[82] M. Escudero, Neutrino decoupling beyond the standard model: CMB constraints on the dark matter mass with a fast and precise $N_{\rm eff}$ evaluation, J. Cosmol. Astropart. Phys. 02 (2019) 007.
[83] X. Chu and J. Pradler, Minimal mass of thermal dark matter and the viability of millicharged particles affecting 21-cm cosmology, Phys. Rev. D **109**, 103510 (2024).
[84] HPQCD Collaboration, $B \to K$ and $D \to K$ form factors from fully relativistic lattice QCD, Phys. Rev. D **107**, 014510 (2023).
[85] NA62 Collaboration, Measurement of the very rare $K^+ \to \pi^+\nu\bar{\nu}$ decay, J. High Energy Phys. 06 (2021) 093.
[86] KOTO Collaboration, Study of the $K_L \to \pi^0\nu\bar{\nu}$ decay at the J-PARC KOTO experiment, Phys. Rev. Lett. **126**, 121801 (2021).
[87] Belle Collaboration, Search for $\mathbf{B \to h\nu\bar{\nu}}$ decays with semileptonic tagging at Belle, Phys. Rev. D **96**, 091101 (2017).
[88] IceCube Collaboration, Search for neutrino lines from dark matter annihilation and decay with IceCube, Phys. Rev. D **108**, 102004 (2023).